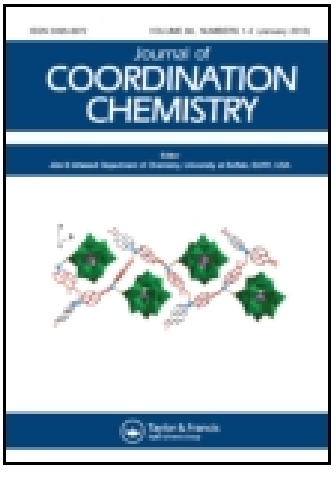

Journal of Coordination Chemistry
Publication details, including instructions for authors and subscription information:
http://www.tandfonline.com/loi/gcoo20

Two new halide-containing polyoxometalate-based compounds

La-Mei Wang[a], Hai-Yang Guo[a], Su Li[a], Yang-Yang Hu[a], Yan Wang[a], Li-Na Xiao[a], De-Chuan Zhao[a], Zhong-Min Gao[a], Da-Fang Zheng[a], Xiao-Bing Cui[a], Yong Fan[a] & Ji-Qing Xu[a]

[a] College of Chemistry and State Key Laboratory of Inorganic Synthesis and Preparative Chemistry, Jilin University, Changchun, China

Accepted author version posted online: 12 Feb 2014.Published online: 05 Mar 2014.

Journal of Coordination Chemistry, 2014
Vol. 67, No. 4, 728–736, http://dx.doi.org/10.1080/00958972.2014.890719

Two new halide-containing polyoxometalate-based compounds

LA-MEI WANG, HAI-YANG GUO, SU LI, YANG-YANG HU, YAN WANG, LI-NA XIAO, DE-CHUAN ZHAO, ZHONG-MIN GAO, DA-FANG ZHENG, XIAO-BING CUI*, YONG FAN* and JI-QING XU

College of Chemistry and State Key Laboratory of Inorganic Synthesis and Preparative Chemistry, Jilin University, Changchun, China

(*Received 21 October 2013; accepted 10 January 2014*)

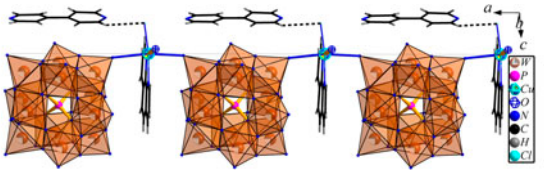

Two new compounds, $[CuCl(Phen)(H_2O)][PW_{12}O_{40}][4,4'\text{-}H_2bpy]\cdot 1.5H_2O$ (**1**) and $[Cd_2(Phen)_4Cl_2][HPMo_{12}O_{40}](4,4'\text{-bpy})$ (**2**) (bpy = bipyridine, Phen = phenanthroline), have been hydrothermally prepared and characterized by IR, UV–vis, XPS, XRD, elemental analysis, cyclic voltammetry analysis, and single-crystal X-ray diffraction analysis. Compound **1** exhibits a 1-D chain structure constructed from polyoxometalates (POMs) and transition metal complexes, whereas **2** presents a supramolecular structure constructed from POMs, metal halide clusters, and organic ligands.

Keywords: Polyoxometalate; Crystal structure; Hydrothermal; Transition metal complexes; Halide-containing compound

1. Introduction

Polyoxometalates (POMs) are molecular metal-oxygen clusters with diverse structures and tunable properties, with applications in analytical chemistry, material science, magnetism, catalysis, and medicine [1–6]. Halide-containing POM-based compounds have been reported by several research groups [7–11]. Roles of halides in POM-based compounds could be divided into three types: (1) halides are templates with no covalent interactions with metal ions [7–9]; (2) halides serve as terminal monodentate ligands [10]; and (3) halides are multidentate ligands [11–16]. The last type is more interesting and important, for multidentate halides will yield metal halide clusters (MHCs).

*Corresponding authors. Email: cuixb@mail.jlu.edu.cn (X.-B. Cui); mrfy@jlu.edu.cn (Y. Fan)

Recently, our group began research in this field and synthesized $[Cu(Phen)_2]_4[Cu_5Cl_4(Phen)_4][XW_{12}O_{40}]_2{\cdot}nH_2O$ (**3**: X = B, $n = 2$; **4**: X = P, $n = 4$) [12], $\{[PMo_{12}Sb_2O_{40}][(Cd(Phen)_2)_2Cl]\}$ (**5**) [13], $[Cd_2(Phen)_4Cl_2][HPW_{12}O_{40}]{\cdot}H_2O$ (**6**) [14], $[BW_{12}O_{40}]_2[Cu_2(Phen)_4Cl](H_2$4,4′-bpy$)_4{\cdot}H_3O{\cdot}5H_2O$ (**7**) [15], $[HPW_{12}O_{40}][Cd_2(Phen)_4Cl_2]$(4,4′-bpy) (**8**) [15], $[Cu(Phen)_2]_4[Cu_5L_4(Phen)_4][XW_{12}O_{40}]{\cdot}nH_2O$ (**9**: L = Cl, X = Al, $n = 4$; **10**: L = Br, X = B, $n = 8$; **11**: L = Br, X = Al, $n = 6$; **12**: L = Br, X = P, $n = 4$) [16], $[Cu(Phen)_2]_4[Cu_4L_3(Phen)_4][XW_{12}O_{40}]{\cdot}nH_2O$ (**13**: L = I, X = B, $n = 3$; **14**: L = I, X = P, $n = 3$) and $[Cu(Phen)_2]_2[Cu_{11}Cl_7(Phen)_8][AsW_{12}O_{40}]$ (**15**) [16] (bpy = bipyridine, Phen = phenanthroline), all of which belong to type (III) halide-containing POM-based compounds. Compounds **5** and **7** are based on di-nuclear MHCs; **6** and **8** are based on di-nuclear MHCs too, but the MHC in **6** and **8** is different from that in **5** and **7**; compounds **3**, **4,** and **9–12** are based on penta-nuclear MHCs; **13** and **14** are based on tetra-nuclear MHCs and **15** is based on undeca-nuclear MHCs. The syntheses of the compounds inspired us to continue work in this field.

In this article, we report the preparations and characterizations of two new halide-containing POM-based compounds, $[CuCl(Phen)(H_2O)][PW_{12}O_{40}][4,4'\text{-}H_2bpy]{\cdot}1.5H_2O$ (**1**) and $[Cd_2(Phen)_4Cl_2][HPMo_{12}O_{40}](4,4'\text{-bpy})$ (**2**). Compound **1** belongs to type II, which contains a transition metal complex (TMC) formed by a metal ion, an organic ligand, a chloride and a water. Compound **2**, which belongs to type III, presents a supramolecular structure constructed from POMs, MHCs, and organic ligands.

2. Experimental

2.1. *General procedures*

All reagents were purchased from commercial sources and were used without purification. Elemental analyses (C, H, N, Mo, W, and P) were performed on a Perkin-Elmer 2400 CHN elemental analyzer and a Perkin-Elmer Optima 3300DV spectrophotometer. Infrared spectra were recorded with a Perkin-Elmer SPECTRUM ONE FTIR spectrophotometer with KBr pellets from 4000 to 200 cm^{-1} and UV–vis spectra were recorded on a Shimadzu UV3100 spectrophotometer using saturated DMF solutions of **1** and **2**. XPS measurement was performed on single crystals with ESCALAB MARK II apparatus using a Mg Kα (1253.6 eV) achromatic X-ray radiation source. All binding energies were referenced to the C1s peak at 284.8 eV of the surface adventitious carbon. Powder XRD patterns were obtained with a Scintag X1 powder diffractometer system using Cu Kα radiation with a variable divergent slit and a solid-state detector. The electrochemical measurements were carried out on a CHI 660B electrochemical workstation. The working electrode was glassy carbon, while the surface of the glassy carbon working electrode was polished with 1 μm alumina and washed with distilled water before each experiment. The counter electrode was a Pt wire and Ag/AgCl served as reference electrode. The measurements were made at 25 °C.

2.2. *Preparation*

2.2.1. Preparation of $[CuCl(Phen)(H_2O)]$ $[PW_{12}O_{40}][4,4'\text{-}H_2bpy]{\cdot}1.5H_2O$ (1). Compound **1** was synthesized hydrothermally by reacting $Na_2WO_4{\cdot}2H_2O$ (0.65 g, 2.0 mM), Sb_2O_3 (0.21 g, 0.71 mM), 85% H_3PO_4 (0.34 g, 3.5 mM), $CuCl_2{\cdot}2H_2O$ (0.23 g, 1.3 mM), 4,4′-bpy (0.05 g, 0.27 mM), Phen (0.07 g, 0.33 mM), and distilled water (15 mL) in a 25 mL Teflon-lined autoclave. The pH was adjusted to 2 with HCl solution. The mixture was

heated under autogenous pressure at 160 °C for 5 days and then left to cool to room temperature. Attempt to isolate **1** by removal of Sb_2O_3 results in unidentified powders. Green crystals could be isolated in 67% yield (based on W). Anal. Calcd for $C_{22}H_{23}CuClN_4O_{42.5}PW_{12}$: P, 0.92; W, 65.67; Cu, 1.89; N, 1.67; C, 7.87; H, 0.69%. Found: P, 0.91; W, 65.86; Cu, 1.91; N, 1.64; C, 7.87; H, 0.70%.

2.2.2. Preparation of $[Cd_2(Phen)_4Cl_2][HPMo_{12}O_{40}]$ (4,4′-bpy) (2). Compound **2** was synthesized hydrothermally by reacting $(NH_4)_3PMo_{12}O_{40}\cdot XH_2O$ (0.482 g, 0.26 mM), $CdCl_2\cdot 2.5H_2O$ (0.458 g, 2.01 mM), $H_2C_2O_4\cdot 2H_2O$ (0.403 g, 3.20 mM), Phen (0.132 g, 0.67 mM), 4,4′-bpy (0.105 g, 0.67 mM), and distilled water (20 mL) in a 25 mL Teflon-lined autoclave. The pH of the mixture was adjusted to 3 with HCl solution. The mixture was heated under autogenous pressure at 160 °C for 5 days and then left to cool to room temperature. Green crystals could be isolated in 59% yield (based on W). Anal. Calcd for $C_{58}H_{41}PCl_2Cd_2N_{10}O_{40}Mo_{12}$:Mo, 38.43; P, 1.03; Cd, 7.50; C, 23.25; H, 1.38; N, 4.68%. Found: Mo, 38.15; P, 0.89; Cd, 7.26; C, 22.47; H, 1.04; N, 4.72%.

2.3. *X-ray crystallographic analysis*

Reflection intensity data for **1** and **2** were measured on a Rigaku R-AXIS RAPID IP diffractometer with graphite monochromated Mo K_α ($\lambda = 0.71073$ Å) radiation. Crystals showed no evidence of crystal decay during data collection. Structures were solved by direct methods and refined with full-matrix least squares on F^2 using SHELXTL-97 crystallographic software package. All non-hydrogen atoms of **1** and **2** were refined anisotropically. Hydrogens of **1** and **2** were set in calculated positions and refined with a riding mode. A summary of the crystallographic data and structure refinements for **1** and **2** is given in table 1 (Supplementary material).

Table 1. Crystal data and structure refinement for **1**, **2,** and **8**.

	1	**2**	**8**
Empirical formula	$C_{22}H_{23}ClCuN_4O_{42.5}PW_{12}$	$C_{58}H_{41}Cd_2Cl_2Mo_{12}N_{10}O_{40}P$	$C_{58}H_{41}Cd_2Cl_2N_{10}O_{40}PW_{12}$
Fw	3359.60	2995.96	4050.88
Crystal system	Monoclinic	Triclinic	Triclinic
Space group	P2(1)/n	P-1	P1
a (Å)	12.7793(3)	11.574(2)	11.567(2)
b (Å)	18.7899(5)	13.009(3)	12.931(3)
c (Å)	20.5623(5)	27.965(6)	13.907(3)
α (°)	90	85.76(3)	85.52(3)
β (°)	92.401(2)	80.70(3)	80.98(3)
γ (°)	90	76.16(3)	76.13(3)
V (Å^3)	4933.1(2)	4032.0(14)	1992.7(7)
Z	4	2	1
D_c (g/cm^3)	4.524	2.468	3.376
μ (mm^{-1})	28.476	2.496	17.941
F (0 0 0)	5888	2856	1812
θ (°)	1.47–28.35	2.98–27.48	1.62–28.40
R(int)	0.0578	0.0775	0.0302
Data/parameters	12,272/757	17,808/1120	11,749/1054
Gof	1.041	1.094	1.032
R_1 [$I > 2\sigma(I)$]	0.0360	0.0795	0.0439
wR_2 (all data)	0.0876	0.2470	0.1274

$R_1 = \Sigma||F_o| - |F_c||/\Sigma|F_o|$; $wR = [\Sigma w(F_o^2 - F_c^2)_2/\Sigma w(F_o^2)^2]^{1/2}$.

3. Results and discussion

3.1. *Crystal structure of 1*

Crystal structure analysis reveals that the asymmetric unit of **1** is composed of $[PW_{12}O_{40}]^{3-}$, $[CuCl(Phen)(H_2O)]^{+}$, $[4,4'\text{-}H_2bpy]^{2+}$, and one and a half lattice waters. $[PW_{12}O_{40}]^{3-}$, displaying the archetypal Keggin structure, can be described as four internally edge-shared triads (W_3O_{13}) corner-shared to each other and disposed tetrahedrally around a central PO_4. P–O and W–O distances of $[PW_{12}O_{40}]^{3-}$ are comparable to previously reported values [14, 15, 17–20]. Bond valence sums (BVS) for tungstens were calculated by using the parameters given by Brown [21]. Results indicate that the formula of $\{PW_{12}O_{40}\}$ in **1** is $[PW^{VI}{}_{12}O_{40}]^{3-}$.

An unusual feature of **1** is that $[CuCl(Phen)(H_2O)]^{+}$ consists of Cu(1) with three different ligands: a Phen, a chloride, and a water. As shown in figure 1, the local coordination geometry around the Cu(1) can be described as an elongated octahedron, with two nitrogens from Phen with Cu–N bond lengths of 1.99(1)–1.994(9) Å, the chloride with the Cu–Cl bond length of 2.246(3) Å, and oxygen from water with Cu–O bond length of 1.99(1) Å forming the octahedral base plane, and two terminal oxygens belonging to two neighboring POMs with Cu–O bond distances of 2.6079(1)–2.6208(1) Å being located at the vertices. The axial Cu–O bond distances are much longer than the Cu–O, Cu–Cl and Cu–N bonds in the octahedral plane, which can be interpreted in terms of Jahn–Teller distortion.

Through axial Cu–O bonds, Cu(1) complexes link neighboring Keggin polyanions $[PW_{12}O_{40}]^{3-}$ to give an unusual $\{[PW_{12}O_{40}][CuCl(Phen)(H_2O)]\}_n$ chain structure with an –ABAB– linking, as shown in figure 2. Alternatively, $[PW_{12}O_{40}]^{3-}$ is utilized as a multidentate ligand, coordinating to two $[CuCl(Phen)(H_2O)]^{+}$ complexes via terminal oxygens to yield an unprecedented 1-D chain structure. The structure of the chain is very interesting. The centers of the POMs and coppers in the chain are not arranged in a straight line running along the *a* axis, as shown in figure 2; the line passing through the metal centers is almost tangent to the surface of the POMs. Phen coordinating to Cu(1) is sandwiched by two neighboring POMs with the oxygens of the POMs to the centers of the aromatic rings

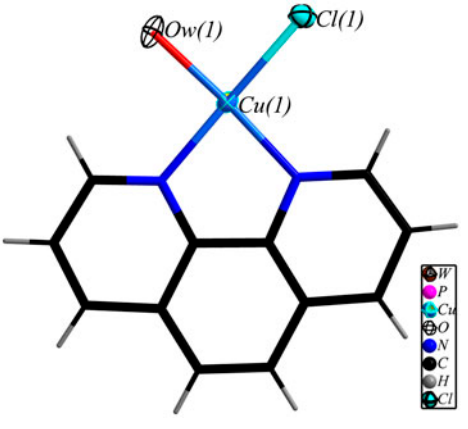

Figure 1. Ball-and-stick and wire representations of the TMC in **1**.

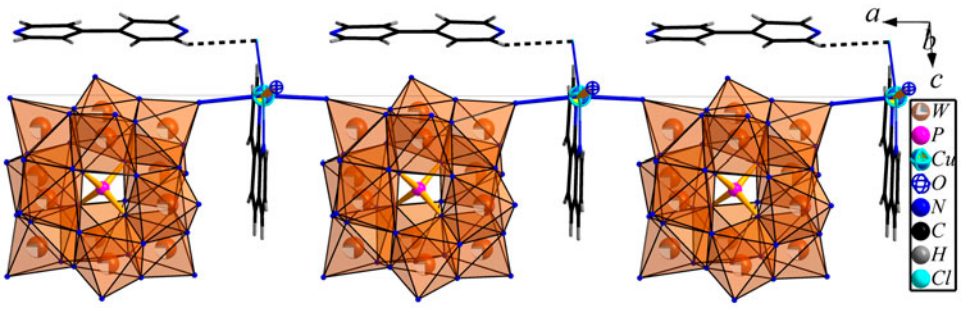

Figure 2. Polyhedral and wire representations of the 1-D chain structure in **1**.

of the Phen at 3.213(8)–3.250(7) Å, indicating that there exist strong lp···π interactions between oxygens and the aromatic rings. The lp···π interactions are the reason that POMs and copper(II)-aqua-chloro-phenanthroline complexes are arranged in such a fashion.

There is a 4,4-bpy ligand, which is just located at a side of a POM with strong C–H···Cl hydrogen bonding between the C(7) of the 4,4-bpy and Cl(1) attached to Cu(1). The C–Cl distance is 3.5961(1) Å, H–Cl distance is 2.8486(1) Å, and the C–H···Cl angle is 138.237 (1)°, meaning strong C–H···Cl hydrogen bonding.

The chain formed by TMCs and POMs can be described as a train structure with each POM as the railroad car. Each hydrogen-bond attached 4,4-bpy looks like a flapping flag attached on each running railroad car along the $-a$ axis. To the best of our knowledge, no extended structure consisting of POMs and such TMCs has been reported previously.

There is only one POM-based compound containing such a copper(II)-aqua-chloro-phenanthroline complex reported by Shivaiah and Das [10]. Our compound is thoroughly different from the Das one. The POM in our compound is a Keggin anion and the POM in the Das case is an Anderson anion; POMs and TMCs in our compound form a novel 1-D chain structure and POMs and TMCs in the Das case form a discrete POM supported TMC.

3.2. *Crystal structure of 2*

The crystallographic study reveals that the asymmetric unit of **2** is comprised of a Keggin anion $[HPMo_{12}O_{40}]^{2-}$, two halves of $[Cd_2(Phen)_4Cl_2]^{2+}$, and a 4,4′-bpy. The anion in **2** is very similar to that in **1**, which also has the Keggin structure. There exist two main differences between **1** and **2**. The most fundamental difference of the two is the metal center of the two Keggin structures, with molybdenum in **2** but tungsten in **1**. The other main difference is that there is crystallographic disorder that leads to the observation of a cube in **2** instead of a tetrahedron on the central PO_4 tetrahedral group in **1**. This is very common for Keggin anions lying on an element of symmetry. All bond lengths are comparable to corresponding bond lengths in reported compounds [13, 20]. BVS for Mo were calculated using the parameters given by Brown [21]. Results indicate that the oxidation state is +6. So the formula is $[HPMo^{VI}{}_{12}O_{40}]^{2-}$.

A feature of **2** is that $[PMo_{12}O_{40}]^{3-}$ is monoprotonated, which means that there would be strong hydrogen bonding interactions between neighboring $[HPMo_{12}O_{40}]^{2-}$. As shown in figure 3, O(31) from POM interacts with O(41a) (a: $-1+x$, y, z) from the neighboring one

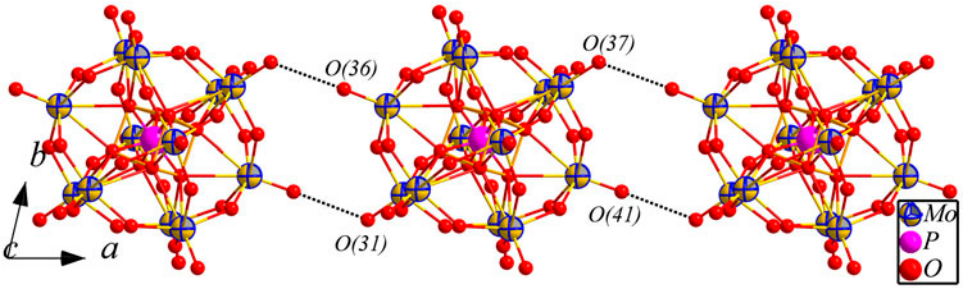

Figure 3. The 1-D supramolecular chain structure connected through O–H···O hydrogen bonding interactions between neighboring POMs in **2**.

with O···O distance of 2.8188(7) Å, while O(36) from the POM interacts with O(37a) (*a*: $-1+x$, *y*, *z*) from the neighboring one with O···O distance of 2.7900(7) Å. The two O···O distances are both in the range of strong O–H···O hydrogen bonding interactions, however, there exists only one hydrogen between the two neighboring POMs, perhaps disordered between O(31), O(41a) and O(36), O(37a) atoms. Alternatively, neighboring monoprotonated $[HPMo_{12}O_{40}]^{2-}$ anions are connected with each other through strong O–H···O hydrogen bonding interactions into an infinite chain structure.

Compound **2** contains $[Cd_2(Phen)_4Cl_2]^{2+}$, each of which is composed of two $[Cd(Phen)_2]^{2+}$ and two chlorides. As shown in figure 4, Cd is coordinated by four nitrogens from two Phen with bond distances of 2.31(1)–2.44(1) Å and by two chlorides with bond distances of 2.588(4)–2.726(4) Å, exhibiting a tetragonal bipyramidal coordination geometry. Each chloride in **2** coordinates to two Cd^{2+} ions with Cd–Cl–Cd angles of 94.7(1)–95.1(1)°, such that chloride adopts a V-shape coordination geometry. The chlorides serve as bridges joining two $[Cd(Phen)_2]^{2+}$ into a metal chloride cluster. Two $[Cd(Phen)_2]^{2+}$ are linked by two chlorides, forming $[Cd_2(Phen)_4Cl_2]^{2+}$.

The MHC $[Cd_2(Phen)_4Cl_2]^{2+}$ in **2** has been reported by our group previously in **6** and **8** [14, 15]. Compounds **2**, **6,** and **8** are very similar. The main difference of **6** and **8** is that **8**

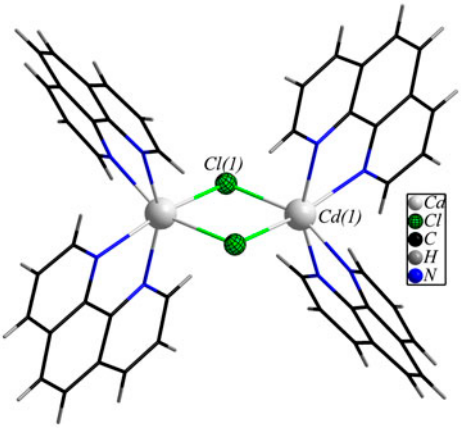

Figure 4. The MHC in **2**.

contains extra 4,4′-bpy ligands; the only difference in composition of **2** and **8** is the metal, however, the structures of **2** and **8** are not isostructural and isomorphous. Compound **2** crystallizes in the triclinic space group P-1 with $a = 11.574(2)$ Å, $b = 13.009(3)$ Å, $c = 27.965(6)$ Å, $\alpha = 85.76(3)°$, $\beta = 80.70(3)°$, and $\gamma = 76.16(3)°$, whereas **8** crystallizes in the triclinic space group P1 with $a = 11.567(2)$ Å, $b = 12.931(3)$ Å, $c = 13.907(3)$ Å, $\alpha = 85.52(3)°$, $\beta = 80.98(3)°$, and $\gamma = 76.13(3)°$. In addition, PLATON suggests the space group P-1 for the structure of **8**. We have attempted to refine the structure in the space group P-1, but the result contains terrible disorder that cannot be solved, thus we have to choose the P1 as the final result for **8**. Furthermore, the space group P1 can be converted to P-1, but the lattice parameters did not change ($a = 11.567(2)$ Å, $b = 12.931(3)$ Å, $c = 13.907(3)$ Å, $\alpha = 85.52(3)°$, $\beta = 80.98(3)°$, $\gamma = 76.13(3)°$). Both the composition and structure of **2** are similar to those of **8**; however, **2** is based on molybdenum but **8** is based on tungsten, and the lattice parameters of the two are different, with the c parameter in **2** approximately twice of that in **8**. The reason why the two can crystallize in the same monoclinic space group P-1 but with different lattice parameters is still elusive.

Though **2** contains a large number of pyridine rings, there exists only one independent $\pi\cdots\pi$ interaction in **2**; the pyridine ring (C(40), C(41), C(42), C(43), C(47), and C(48)) interacts with its symmetry equivalent through $\pi\cdots\pi$ interaction with face to face distance of 3.7942 Å.

The dissociated 4,4′-bpy in **2** is not protonated, thus we speculate that there should be no N–H···O hydrogen bonding interactions in **2**. The crystallographic result confirms our speculation with the shortest N···O distance in **2** of 3.1610(8) Å. There exists only one independent C–H···O hydrogen bonding interaction in **2**, which is C(39)–H(39)···O(43) with C···O distance of 3.126(1) Å.

3.3. *Properties*

XRD patterns for **1** and **2** are in agreement with the ones simulated based on the data of single-crystal X-ray structures (figure S1, see online supplemental material at http://dx.doi.org/10.1080/00958972.2014.890719), indicating the purity of synthesized products. The differences in reflection intensity of XRD patterns for **1** and **2** are probably due to preferred orientations in the powder samples of **1** and **2**.

The infrared spectrum of **1** shows four characteristic vibrations resulting from Keggin anion: 1079 cm^{-1} typical of the $\nu(P–O_c)$ frequency, 976, 893, and 803 cm^{-1} of the $\nu(W–O_t)$, the $\nu(O_b–W–O_b)$ and the $\nu(O_c–W–O_c)$ frequencies, respectively. In addition, absorptions at 1244–1607 cm^{-1} are proof of 4,4′-bpy and 1,10-Phen (figure S2). The infrared spectrum of **2** is similar to that of **1**, also exhibiting four bands of the Keggin anion: 1062 cm^{-1} typical of the $\nu(P–O_c)$ frequency, 956, 880, and 793 cm^{-1} of the $\nu(Mo–O_t)$, the $\nu(O_b–Mo–O_b)$ and the $\nu(O_c–Mo–O_c)$ frequencies, respectively. Absorptions at 1102–1592 cm^{-1} are the proof of 4,4′-bpy and 1,10-Phen in **2** (figure S2).

The XPS spectrum of **1** gives two peaks at 37.6 and 35.4 eV in the W4f region ascribed to W^{6+} (figure S3). The XPS spectrum of **2** gives two peaks at 236.1 and 233.0 eV in the Mo4f region due to Mo^{6+} (figure S3). The XPS estimation of the valence-state values seems to be in reasonable agreement with those calculated from bond valence sum calculations. The results further confirm the W^{6+} and Mo^{6+}.

The UV–vis spectrum at 260–600 nm of **1** is presented in figure S4, displaying a broad medium intense absorption at 267 nm and a shoulder at 295 nm, assigned to O→W charge transfer in the polyoxoanion structure. The UV–vis spectrum of **2** is similar to that of **1**

(figure S4), which also displays a broad medium intensity absorption at 267 nm and a shoulder at 295 nm, assigned to O→Mo charge transfer in the polyoxoanion.

Figure S5 shows the cyclic voltammogram of saturated DMSO solution of **1** in 0.3 M L^{-1} H_2SO_4 at the scan rate of 100 mV s^{-1}. From + 600 to −800 mV, three pairs of redox peaks appear and the peak potentials $E_{1/2} = (E_{pa} + E_{pc})/2$ were −29(I–I′), −349(II–II′) and −625(III–III′) mV, respectively. Redox peaks I–I′ and II–II′ correspond to two consecutive one electron processes of W, while III–III′ corresponds to a two-electron process [22,20].

The cyclic voltammogram of saturated DMSO solution of **2** in 0.3 ML^{-1} H_2SO_4 solution at the scan rate of 100 mV s^{-1} from +400 to −200 mV (figure S5) shows three reversible redox peaks I–I′, II–II′, and III–III′ with the half-wave potentials ($E_{1/2} = (E_{pa} + E_{pc})/2$) at +343(I–I′), +202(II–II′), −36(III–III′) mV, respectively. Redox peaks I–I′, II–II′, and III–III′ correspond to three consecutive two-electron processes of Mo centers [23].

4. Conclusion

Compounds **1** and **2** are two new examples of halide-containing POM-based hybrids. Compound **1** contains a TMC formed by a metal ion, an organic ligand, a chloride, and a water. Compound **2** presents a supramolecular structure constructed from POMs, MHCs, and organic ligands. Both **1** and **2** are new examples of the family of hybrids based on POMs and MHCs. We hope to collect enough examples and find the influence of halide to the structures and properties of this kind of hybrids.

Supplemental material

CCDC numbers: 880878 for **1**; 931064 for **2**. The data can be obtained free ofcharge from the Cambridge Crystallographic Data Center via www.ccdc.cam.ac.uk/data_request/cif.

Funding

This work was supported by the National Natural Science Foundation of China under [grant number 21003056].

References

[1] M.T. Pope. *Heteropoly and Isopoly Oxometalates*, Springer-Verlag, Berlin (1983).
[2] M.T. Pope, A. Müller. *Angew. Chem. Int. Ed. Engl.*, **30**, 34 (1991).
[3] M.T. Pope, A. Müller. *Polyoxometalates: From Platonic Solids to Anti-Retro Viral Activity*, Kluwer, Dordrecht (1994).
[4] C.L. Hill (Ed.), *Chem. Rev.*, **98**, 1 (1998).
[5] M.T. Pope, A. Müller. *Polyoxometalate Chemistry: From Topology via Self-Assembly to Applications*, Kluwer, Dordrecht (2001).
[6] T. Yamase, M.T. Pope. *Polyoxometalate Chemistry for Nano-Composite Design*, Kluwer, Dordrecht (2002).
[7] A. Müller, R. Sessoli, E. Krickemeyer, H. Bögge, J. Meyer, D. Gatteschi, L. Pardi, J. Westphal, K. Hovemeier, R. Rohlfing, J. Döring, F. Hellweg, C. Beugholt, M. Schmidtmann. *Inorg. Chem.*, **36**, 5239 (1997).
[8] S.S. Mal, U. Kortz. *Angew. Chem. Int. Ed.*, **44**, 3777 (2005).

[9] S.S. Mal, B.S. Bassil, M. Ibrahim, S. Nellutla, J.V. Tol, N.S. Dalal, J.A. Fernándaz, X. López, J.M. Poblet, R.N. Biboum, B. Keita, U. Kortz. *Inorg. Chem.*, **48**, 11636 (2009).
[10] V. Shivaiah, S.K. Das. *Inorg. Chem.*, **44**, 8846 (2005).
[11] J. Hua, Y.F. Qi, E.B. Wang, Y.G. Li, C. Qin, X.L. Wang, S. Chang. *Eur. J. Inorg. Chem.*, **22**, 4541 (2006).
[12] L.N. Xiao, Y. Wang, C.L. Pan, J.N. Xu, T.G. Wang, H. Ding, Z.M. Gao, D.F. Zheng, X.B. Cui, J.Q. Xu. *CrystEngComm*, **13**, 4878 (2011).
[13] L.N. Xiao, Y. Peng, Y. Wang, J.N. Xu, Z.M. Gao, Y.B. Liu, D.F. Zheng, X.B. Cui, J.Q. Xu. *Eur. J. Inorg. Chem.*, **12**, 1997 (2011).
[14] Y. Wang, B. Zou, L.N. Xiao, N. Jin, Y. Peng, F.Q. Wu, H. Ding, T.G. Wang, Z.M. Gao, D.F. Zheng, X.B. Cui, J.Q. Xu. *J. Solid State Chem.*, **184**, 557 (2011).
[15] L.M. Wang, Y. Fan, Y. Wang, L.N. Xiao, Y.Y. Hu, Y. Peng, T.G. Wang, Z.M. Gao, D.F. Zheng, X.B. Cui, J.Q. Xu. *J. Solid State Chem.*, **191**, 257 (2012).
[16] L.N. Xiao, Y.Y. Hu, L.M. Wang, Y. Wang, J.N. Xu, H. Ding, X.B. Cui, J.Q. Xu. *CrystEngComm*, **13**, 8589 (2012).
[17] J. Wu, Y.L. Xu, K. Yu, Z.H. Su, B.B. Zhou. *J. Coord. Chem.*, **66**, 2821 (2013).
[18] X. Gan, X.X. Hu, Z.F. Shi, Y.Z. Yin. *J. Coord. Chem.*, **66**, 2930 (2013).
[19] S.H. Yang, X.Q. Dong, Y.P. Zhang, H.M. Hu, G.L. Xue. *J. Coord. Chem.*, **66**, 1529 (2013).
[20] Y.B. Liu, Y. Wang, L.N. Xiao, Y.Y. Hu, L.M. Wang, X.B. Cui, J.Q. Xu. *J. Coord. Chem.*, **65**, 4342 (2012).
[21] I.D. Brown, In *Structure and Bonding in Crystals*, M. O'Keefe, A. Navrotsky (Eds), Vol. 2, pp. 1–30, Academic Press, New York (1981).
[22] A.X. Tian, J. Ying, J. Peng, J.Q. Sha, Z.M. Su, H.J. Pang, P.P. Zhang, Y. Chen, M. Zhu, Y. Shen. *Cryst. Growth Des.*, **10**, 1104 (2010).
[23] X.L. Wang, C. Qin, E.B. Wang, Z.M. Su, Y.G. Li, L. Xu. *Angew. Chem. Int. Ed.*, **45**, 7411 (2006).